EFFECT OF SEX AND INTRAUTERINE GROWTH RESTRICTION ON EPIGENETIC DETERMINANTS IN RAT SUBCUTANEOUS ADIPOSE TISSUE

by

Emily Suzanne Riddle

A thesis submitted to the faculty of
The University of Utah
in partial fulfillment of the requirements for the degree of

Master of Science

in

Nutrition

College of Health

The University of Utah

May 2014

The University of Utah Graduate School

STATEMENT OF THESIS APPROVAL

The thesis of **Emily Suzanne Riddle**

has been approved by the following supervisory committee members:

Lisa Joss-Moore	, Chair	**3/5/14** Date Approved
Julie Metos	, Member	**3/5/14** Date Approved
Kristine Jordan	, Member	**3/5/14** Date Approved

and by **Julie Metos** , Chair/Dean of

the Department/College/School of **Nutrition**

and by David B. Kieda, Dean of The Graduate School.

ABSTRACT

Intrauterine growth restriction (IUGR) predisposes individuals to adult diseases, including obesity. Although IUGR infants are born smaller than their appropriately grown counterparts, fat deposition in IUGR children is accelerated throughout childhood. Storage of excess lipid in the subcutaneous adipose tissue (SAT) protects against ectopic fat deposition in the liver, muscle, and visceral adipose tissue (1). However, if SAT becomes dysfunctional, as evidenced by an increase in the release of pro-inflammatory cytokines as well as activation of the unfolded protein response (UPR), visceral adipose tissue (VAT) is preferentially deposited. Fat deposition in IUGR children favors the formation of VAT over SAT. Failure of SAT to adequately expand in IUGR individuals suggests dysfunction in the SAT depot.

Our group previously demonstrated that IUGR induces SAT dysfunction in male, but not female, weanling rat pups. Early onset adaptations of specific genes regulating SAT, including PPARγ2, may be altered in response to an unfavorable *in utero* environment. In 3T3L1 cell culture, a positive feedback loop has been proposed in which PPARγ2 activates the transcription of the Setd8 gene. Setd8, a lysine methyltransferase, monomethylates H4K20, which further increases transcription of PPARγ2 and PPARγ2 target genes. However, the presence of this feedback loop *in vivo* in adipose tissue remains unknown. Furthermore, sex differences in basal levels of PPARγ2-Setd8-

H4K20Me in male and female control rat pups and the effect of IUGR on the PPARγ2-Setd8-H4K20Me feedback loop are unknown.

We hypothesized that basal regulation of the PPARγ2-Setd8-H4K20Me loop would be different between male and female control rat pups. We also hypothesized IUGR would alter the PPARγ2-Setd8-H4K20Me positive feedback loop in male, but not female, d21 SAT prior to the onset of obesity.

To test this hypothesis, we used a well-characterized rat model of uteroplacental insufficiency-induced IUGR. Our study demonstrated that sex differences exist between basal levels of PPARγ2-Setd8-H4K20Me in male and female control rat pups. Our results also demonstrated that IUGR dysregulates the PPARγ2-Setd8-H4K20Me positive feedback loop in a sex-specific manner, with the majority of molecular effects confined to male rat pups. Our sex-specific molecular observations may partially explain the varying responses of male and female adipose tissue to IUGR.

TABLE OF CONTENTS

LIST OF FIGURES

ACKNOWLEDGEMENTS

I would like to express my immeasurable appreciation and deepest gratitude to my thesis advisor, Dr. Lisa-Joss Moore, for her constant insight and support. I am very grateful for the opportunities that Dr. Joss-Moore has made available to me over the past two years. Dr. Joss-Moore is a true role model, whose actions I aspire to emulate for years to come.

I would also like to thank my committee members, Dr. Julie Metos and Dr. Kristine Jordan, for their guidance and encouragement throughout this thesis process.

Finally, I need to thank my family for their endless love. I would not be who I am today without their inspiration and support.

INTRODUCTION

Uteroplacental insufficiency secondary to maternal hypertension is a common complication of pregnancy and is a leading cause of intrauterine growth restriction (IUGR) in developed countries (2-4). In uteroplacental insufficiency-induced IUGR, reductions in blood flow to the fetus restrict growth and inhibit the fetus from achieving its *in utero* genetic growth potential.

IUGR predisposes individuals to adult-onset disease, including obesity (5-8). Although IUGR infants are born smaller than their appropriately grown counterparts, the rate of adipose deposition in IUGR infants is accelerated throughout childhood (6, 9). Storage of excess lipid in the subcutaneous adipose tissue (SAT) protects against ectopic fat deposition in the liver, muscle, and visceral adipose tissue (1, 10). Despite SAT and visceral adipose tissue (VAT) both consisting primarily of adipocytes, SAT and VAT contribute differently to the development of metabolic disorders; SAT is protective while VAT is detrimental (11). If SAT becomes dysfunctional, as evidenced by an increase in the release of pro-inflammatory cytokines as well as activation of the unfolded protein response (UPR)(12), VAT is preferentially deposited. Fat deposition in IUGR children favors the formation of VAT over SAT (13). Failure of SAT to adequately expand in IUGR individuals suggests dysfunction in the SAT depot.

Using a well-defined rat model of IUGR, our group demonstrated that IUGR induces SAT dysfunction in male, but not female, weanling rat pups (14). This SAT

dysfunction is evidenced by increased expression of the pro-inflammatory cytokine TNF-α, as well as activation of the UPR (15). Increased ectopic accumulation of muscle triglycerides (16) and VAT (14) also accompany this sex-specific SAT dysfunction. An important concept is that the observed SAT dysfunction in males, but not females, takes place *prior* to the onset of overt obesity; i.e., at a time when IUGR rat pups still weigh less than controls.

Early onset adaptations of specific genes regulating SAT may be altered in response to an unfavorable *in utero* environment. These early onset adaptations alter the basal regulation of specific genes, thereby changing the way these genes respond to various environments and insults throughout the life span (17). This phenomenon is also referred to as programming. One candidate gene for programming is PPARγ.

PPARγ is a member of the nuclear receptor family of transcription factors. At least two isoforms, PPARγ1 and PPARγ2, can be made from the PPARγ gene (18). Both isoforms are involved in the regulation of genes required for cell differentiation and proliferation (19). However, PPARγ2 is the predominant isoform found in adipose tissue, where it activates target genes involved in adipose differentiation, lipid uptake, and energy homeostasis (19).

In 3T3L1 cell culture, PPARγ2 has been shown to regulate the transcription of the Setd8 gene (20). Setd8 is a lysine methyltransferase and is solely responsible for the placement of the epigenetic mono-methyl mark on histone 4 lysine 20 (H4K20Me). Epigenetic modifications, such as H4K20Me, alter expression of target genes without changing the underlying DNA sequence and are influenced by the environment (17). In adipose cell lines, H4K20Me is associated with increased expression in 85% of the target

genes modified by the mark, suggesting a role in transcriptional activation (20).

A positive feedback loop has been proposed in which H4K20Me coordinates the regulation of adipogenesis through transcriptional activation of PPARγ2 and PPARγ2 target genes, such as Fabp4 and Cd36 (20). PPARγ2 activates the transcription of the Setd8 gene. Setd8 in turn monomethylates H4K20, which further increases the transcription of PPARγ2 and PPARγ2 target genes (Figure 1).

This feedback loop has only been shown in 3T3L1 cell culture, and its presence *in vivo* in adipose tissue is not known. Furthermore, sex differences in basal levels of PPARγ2-Setd8-H4K20Me in male and female control rat pups are unknown. Also, the density of the H4K20Me mark at different locations along the PPARγ2 gene, and the effect of IUGR on the PPARγ2-Setd8-H4K20Me positive feedback loop are unknown.

We hypothesized that basal regulation of the PPARγ2-Setd8-H4K20Me loop would be different between male and female control rat pups. We also hypothesized IUGR would alter the PPARγ2-Setd8-H4K20Me positive feedback loop in male, but not female, d21 SAT prior to the onset of obesity.

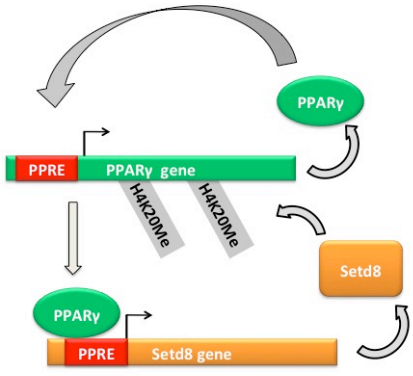

Figure 1 PPARγ2-Setd8-H4K20Me Positive Feedback Loop

METHODS

Rat Model

All procedures were approved by the University of Utah Animal Care Committee and are in accordance with the American Physiological Society's guiding principles (21). IUGR was induced by rat uteroplacental insufficiency. Briefly, on day 19 of gestation, pregnant Sprague-Dawley rats were anesthetized with intraperitoneal xylazine (8 mg/kg) and ketamine (40 mg/kg). Both uterine arteries were ligated, giving rise to IUGR pups. Control dams underwent identical anesthetic procedures. After maternal rats delivered spontaneously at term, pups were weighed and litters randomly culled to 6 pups. Pups remained with the dam and were fed via lactation until postnatal day 21 (d21). Rat pups were killed at d21, and SAT was collected for RT-PCR and Western blotting or chromatin immunoprecipitation.

Real-time RT-PCR

Real-time reverse transcriptase polymerase chain reaction (RT-PCR) was used to evaluate PPARγ2, and Setd8 mRNA abundance in male and female d21 SAT. Total RNA was extracted from frozen control and IUGR SAT using the RNeasy Lipid Tissue Kit (Qiagen). Total RNA was quantified using the Epoch Microplate Spectrophotometer (Biotek). cDNA was synthesized using a High Capacity cDNA Reverse Transcription Kit (Applied Biosystems) from 1 ug of total RNA. The following Assay-on-demand primer/probe sets were used: PPARγ2 – Rn00440940_m1, and Setd8 – Rn01477383_q1. GAPDH was used as an internal control (GAPDH primer and probe sequences. Forward:

CAAGATGGTGAAGGTCGGTGT; Reverse: CAAGAGAAGGCAGCCCTGGT; Probe: GCGTCCGATACGGCCAAATCCG). mRNA levels were determined using the comparative Ct method (22). All RT-PCR amplification, data acquisition, and analysis were done using the QuantiStudio 12K Flex Real Time PCR system using a 384-well Optical Reaction Plate (Applied Biosystems). TaqMan Universal PCR Master Mix II with UNG (Applied Biosystems) was used in a 6 uL reaction performed in quadruplicate. Cycle parameters were: 50°C x 2 minutes, 95°C x 10 minutes, followed by 40 cycles of 95°C x 15 seconds and 60°C x 60 seconds.

Western Blotting

Western blotting was used to evaluate PPARγ2 and Setd8 protein abundance in male and female d21 SAT. Briefly, total protein was isolated by homogenizing SAT in RIPA buffer (50 mM Tris‑HCl, pH 8.0, 150 mM NaCl, 0.5% Na-deoxy-cholate, 1% NP-40 (Igepal), and 0.1% SDS) and protease inhibitor (PI) cocktail (Roche-Complete Mini). Samples were centrifuged, and supernatants were collected and stored at – 80°C until use. Cytoplasmic protein was isolated by suspending SAT in buffer A (10mM Hepes pH 7.9, 10 mM KCl, 0.1 mM EDTA pH 8.0, 1.5 mM $MgCl_2$, 1.0 mM DTT, 0.5 mM PMSF, 1x PI) and douncing samples. Samples were centrifuged and the cytoplasmic supernatant was transferred to a new 1.7 mL tube. Nuclear protein was isolated by resuspending the pellet in buffer C (20 mM HEPES pH 7.9, 0.4 M NaCl, 1.0 mM EDTA, 1.5 mM $MgCl_2$, 1.0 mM EGTA, 1.0 mM DTT, 1.0 mM PMSF, 10% glycerol, 1 x PI). Samples were homogenized with a Fisher homogenizer and then centrifuged. The nuclear supernatant was transferred to a new 1.7 mL tube. Protein levels were quantified using the Pierce BCA protein assay kit (ThermoScientific) and were stored at -80°C until use.

Cytoplasmic (25 ug), nuclear (25 ug), or total (30 ug) protein was loaded and separated on Nu-PAGE 10% Bis-Tris Midi Gels (Novex by Life Technologies). Proteins were transferred to PVDF membranes (Milli-pore). PVDF membranes were blocked in 5% milk-TBST, and primary antibodies were diluted 1:500 (PPARγ), 1:300 (Setd8), or 1:5000 (GAPDH) in 5% milk-TBST. The following primary antibodies were used: PPARγ (H-100, Santa Cruz Biotechnology), Setd8 (Q-18, Santa Cruz Biotechnology), and GAPDH (14C10, Cell Signaling Technology). Blots were incubated overnight at 4°C then probed with the appropriate secondary antibody: anti-rabbit secondary antibody (Cell Signaling Technology) or anti-goat secondary antibody (Santa Cruz Biotechnology). Antibodies were detected with Western Lightning enhanced chemiluminescence and quantified using an Image Station 2000R (Eastman Kodak).

Chromatin Isolation and Quantification

A revised ChIP protocol, based on the methods of Nelson et al. (23), was used to isolate and quantify chromatin in male and female d21 SAT. Briefly, SAT was fixed in 1% formaldehyde for 5 minutes at room temperature. Cross-linking was quenched with the addition of glycine to a final concentration of 0.125 M. After centrifugation, the pellet and intermediate liquid phase were aspirated using a Pasteur pipette. The upper phase was washed twice with ice-cold PBS supplemented with 1x PI followed by centrifugation. After the second wash, samples were resuspended in cell lysis buffer (5mM PIPES pH 8.0, 85 mM KCL, 0.5% NP40, 1x PI) and incubated on ice. Each sample was dounced on ice for 5 minutes and transferred to a new 1.7 mL tube. After centrifugation, the supernatant was discarded. The pelleted nuclei were resuspended in nuclei lysis buffer (50 mM Tris-CL pH 8.1, 10 mM EDTA, 1% SDS, 1x PI), incubated

on ice for 15 minutes, and sonicated using a Fisher Scientific Sonic Model 100 Dismembrator. Each sample was sonicated for 20 seconds at 40% power then returned to ice. Samples underwent 15 rounds of sonication. After centrifuging, the supernatant was collected and split into three 1.7 mL tubes (50 uL input, 150 uL antibody, 150 uL IgG).

The 50 uL input supernatant was added to195 uL ChIP Buffer 2 (ChIP-IT Express Kit, Active Motif) and 5 uL 5M NaCl, so that the final volume was 250 uL. Tubes were boiled at 95°C for 15 minutes. Tubes were returned to room temperature, and 1 ug proteinase K was added to each tube. Tubes were incubated in a 55°C water bath for 45 minutes. After incubation, proteinase K stop solution was added to each tube, and the DNA was purified using the Qiagen QIAquick PCR Purification Kit. Input DNA concentration was determined using the Epoch Microplate Spectrophotometer (Biotek). One ug of chromatin was run on a 1.5% agarose gel to determine chromatin size.

Chromatin Immunoprecipitation

Chromatin immunoprecipitation was used to evaluate the levels of H4K20Me along the PPARγ gene in male and female d21 SAT. The following positions were analyzed: Promoter 1 (P1), Promoter 2 (P2), Exon 1, and Exon 4. Promoter 1 (P1) is specific to PPARγ1, and promoter 2 (P2) is specific to PPARγ2. Both isoforms share exons 1 - 6 within the body of the gene (Figure 2).

The ChIP-IT Express kit (Active Motif) was used for all immunoprecipitation reactions. Ten to twenty ug of chromatin was used for each reaction. The following antibodies were used for the immunoprecipitation reactions: H4K20Me antibody (Novus Biologicals), Rabbit IgG antibody (Santa Cruz Biotechnology). Primer sequences used for RT-PCR of IP DNA are listed in Table 1 (see Appendix).

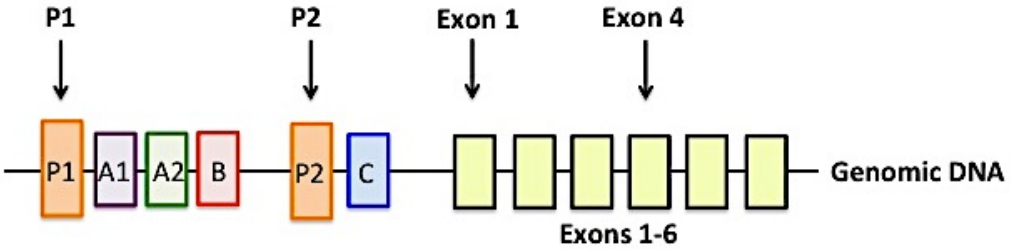

Figure 2 PPARγ Gene

Statistical Analysis

Female control groups were compared to male control groups. IUGR groups were compared to the corresponding sex-matched control. Statistical significance was determined by Mann-Whitney U using the StatView 5 software package (SAS Institute, Inc.). $P \leq 0.05$ was considered significant. For all experiments, 6 rats per group (control male, control female, IUGR male, and IUGR female) were randomly selected from different litters. We chose a sample size of 6 per group for our experiments based on previous studies from our lab demonstrating that a sample size of 6 per group was sufficient to detect differences of 10% expression of mRNA and protein.

RESULTS

Sex-Based Differences in PPARγ2-Set8-H4K20Me

This section will compare control males to control females to determine basal sex differences in the PPARγ2-Set8-H4K20Me loop. PPARγ2 and Setd8 mRNA levels were measured in male and female control d21 rats. Female control PPARγ2 mRNA was significantly increased relative to male control PPARγ2 mRNA ($p = 0.003$) (Figure 3A). Female control Setd8 mRNA was also significantly increased compared to male control Setd8 mRNA ($p = 0.003$) (Figure 3B). Male and female PPARγ2 and Setd8 protein levels could not be compared because samples were run on separate blots.

H4K20Me levels were measured along the PPARγ gene in male and female control d21 SAT. Female levels of H4K20Me were significantly increased when compared to male levels of H4K20Me at Exon 1 ($p = 0.01$) and Exon 4 ($p = 0.01$) (Figure 4). However, female levels of H4K20Me were not significantly different than male levels of H4K20Me at P1 or P2 (Figure 4).

Figure 3 Sex Differences in Control PPARγ2 and Setd8 mRNA
* Denotes statistically different to male, $p \leq 0.05$.

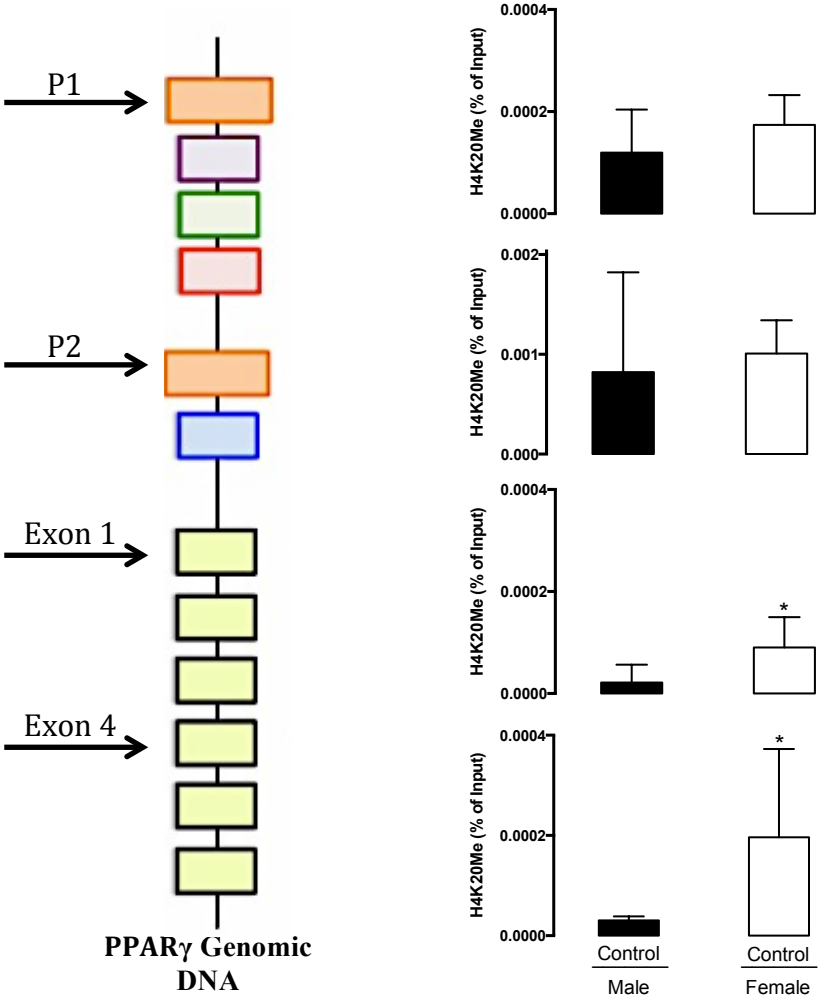

Figure 4 Sex Differences in H4K20Me along PPARγ
* Denotes statistically different to male, $p \leq 0.05$.

Effect of IUGR on PPARγ2-Setd8-H4K20Me

This section will compare IUGR rat pups to sex-matched controls to determine the effect of IUGR on the PPARγ2-Set8-H4K20Me loop. Levels of PPARγ2 mRNA were measured in control and IUGR rat pups at d21. In male rat pups, IUGR significantly *increased* PPARγ2 mRNA levels relative to male controls ($p = 0.01$) (Figure 5A). In female rat pups, IUGR significantly *decreased* PPARγ2 mRNA levels relative to female controls ($p = 0.01$) (Figure 5B).

Total, cytoplasmic, and nuclear PPARγ2 protein levels were measured in control and IUGR rat pups at d21. In male rat pups, IUGR did not significantly alter total PPARγ2 protein abundance (Figure 6), but IUGR did significantly decrease cytoplasmic PPARγ2 protein abundance ($p = 0.02$) (Figure 7A). IUGR did not significantly alter nuclear PPARγ2 protein abundance (Figure 7B). However, IUGR did significantly decrease the cytoplasmic to nuclear ratio of PPARγ2 protein in male rat pups ($p = 0.04$) (Figure 7C). In female rat pups, IUGR did not significantly alter total, cytoplasmic (Figure 7D), or nuclear PPARγ2 (Figure 7E) protein abundance. IUGR also did not significantly alter the cytoplasmic to nuclear protein ratio (Figure 7F).

Levels of Setd8 mRNA and protein were measured in male and female rat pups at d21. In male rat pups, IUGR significantly increased Setd8 mRNA levels relative to male controls ($p = 0.006$) (Figure 8A). In female rat pups, IUGR did not significantly alter Setd8 mRNA levels relative to female controls (Figure 8B). IUGR did not significantly alter Setd8 protein levels in male (Figure 9A) or female (Figure 9B) rat pups.

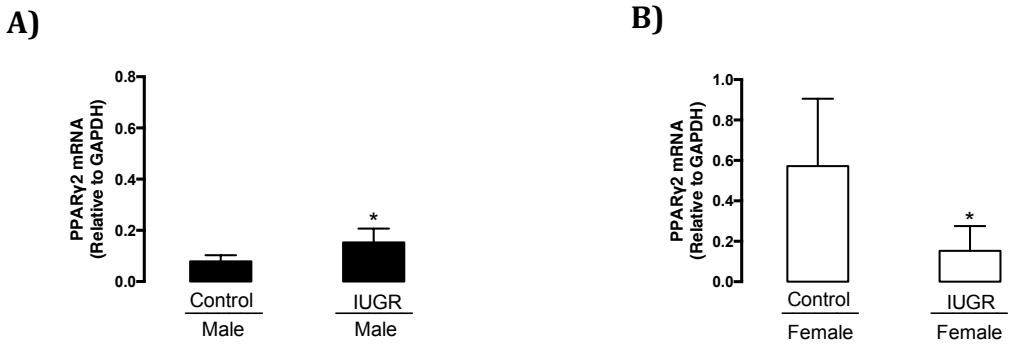

Figure 5 Effect of IUGR on PPARγ2 mRNA
A) Male PPARγ2 mRNA levels relative to GAPDH. B) Female PPARγ2 mRNA levels relative to GAPDH. * Denotes statistical significance relative to sex-matched controls, $p \leq 0.05$.

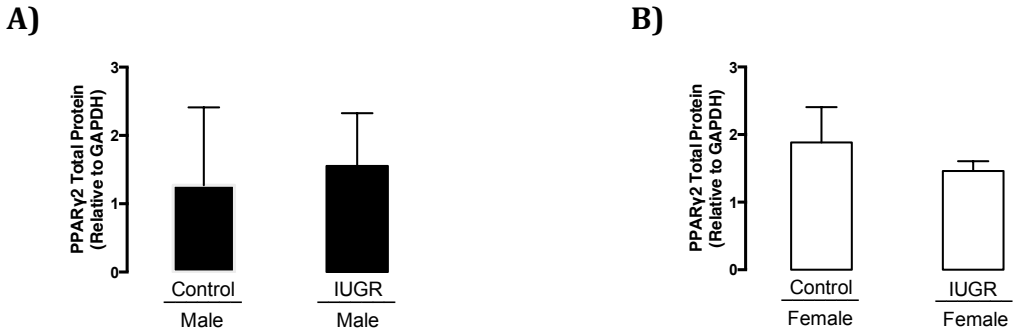

Figure 6 Effect of IUGR on Total PPARγ2 Protein
A) Male PPARγ2 total protein levels relative to GAPDH. B) Female PPARγ2 total protein levels relative to GAPDH. *Denotes statistical significance relative to sex-matched controls, $p \leq 0.05$.

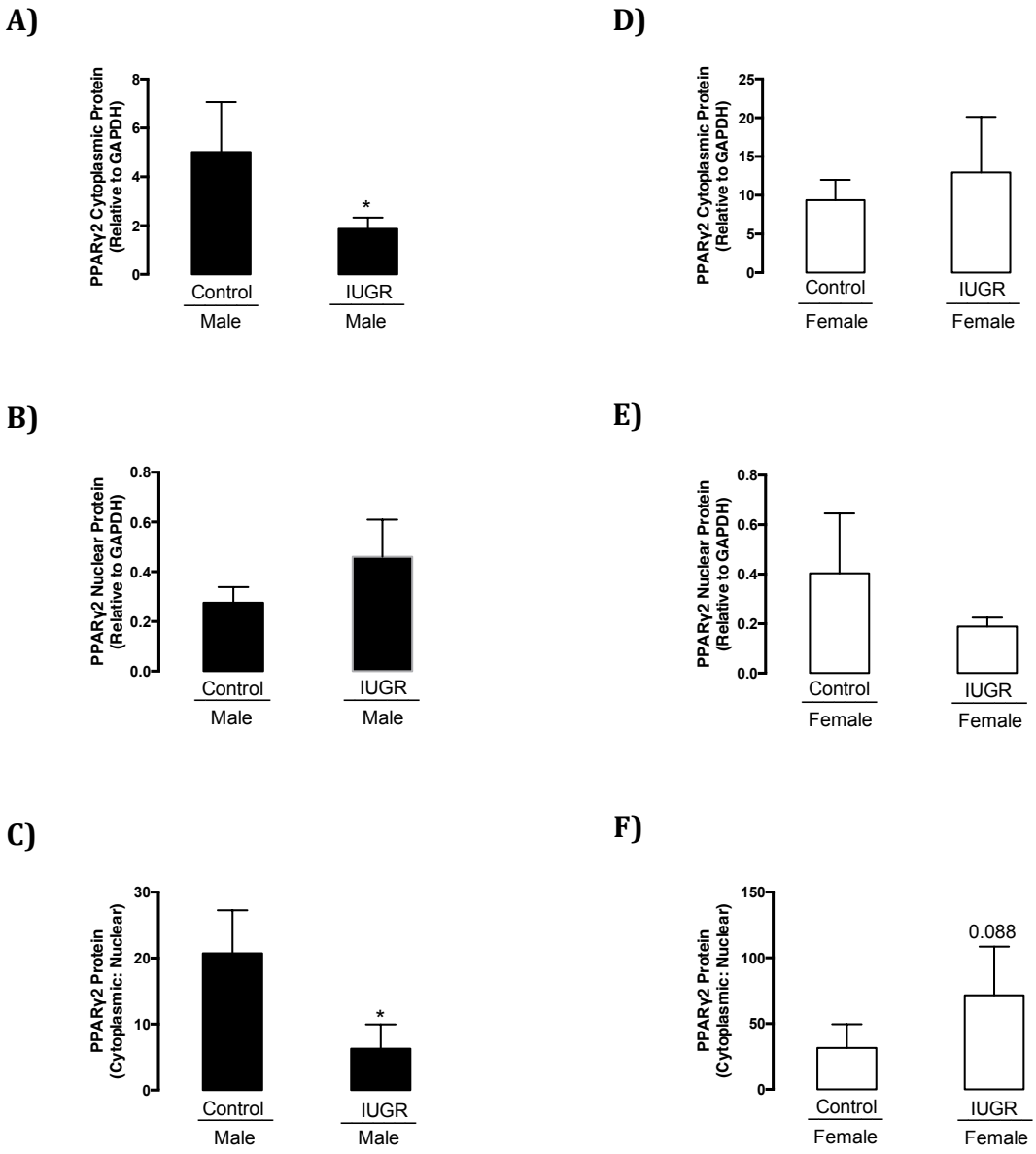

Figure 7 Effect of IUGR on Cytoplasmic and Nuclear PPARγ2 Protein
A) Male cytoplasmic PPARγ2 protein relative to GAPDH. B) Male nuclear PPARγ2 protein relative to GAPDH. C) Male cytoplasmic to nuclear PPARγ2 protein ratio. D) Female cytoplasmic PPARγ2 protein relative to GAPDH. E) Female nuclear PPARγ2 protein relative to GAPDH. F) Female cytoplasmic to nuclear PPARγ2 protein ratio.
* Denotes statistical significance relative to sex-matched controls, $p \leq 0.05$.

Figure 8 Effect of IUGR on Setd8 mRNA
A) Male Setd8 levels relative to GAPDH. B) Female Setd8 levels relative to GAPDH.
* Denotes statistical significance relative to sex-matched controls, $p \leq 0.05$

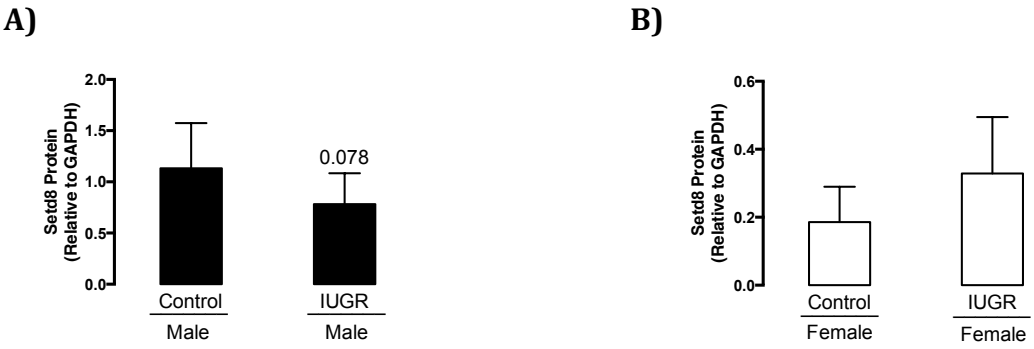

Figure 9 Effect of IUGR on Setd8 Protein
A) Male Setd8 protein levels relative to GAPDH. B) Female Setd8 protein levels relative to GAPDH. * Denotes statistical significance relative to sex-matched controls, $p \leq 0.05$.

Levels of H4K20Me were evaluated at four locations along the PPARγ gene in control and IUGR rat pups at d21. In male rat pups, IUGR significantly increased H4K20Me at Exon 4 ($p = 0.04$) (Figure 10). However, IUGR did not significantly alter levels of H4K20Me at P1, P2, or Exon 1 (Figure 10). In female rat pups, IUGR did not significantly alter levels of H4K20Me at P1, P2, Exon 1, or Exon 4 (Figure 10).

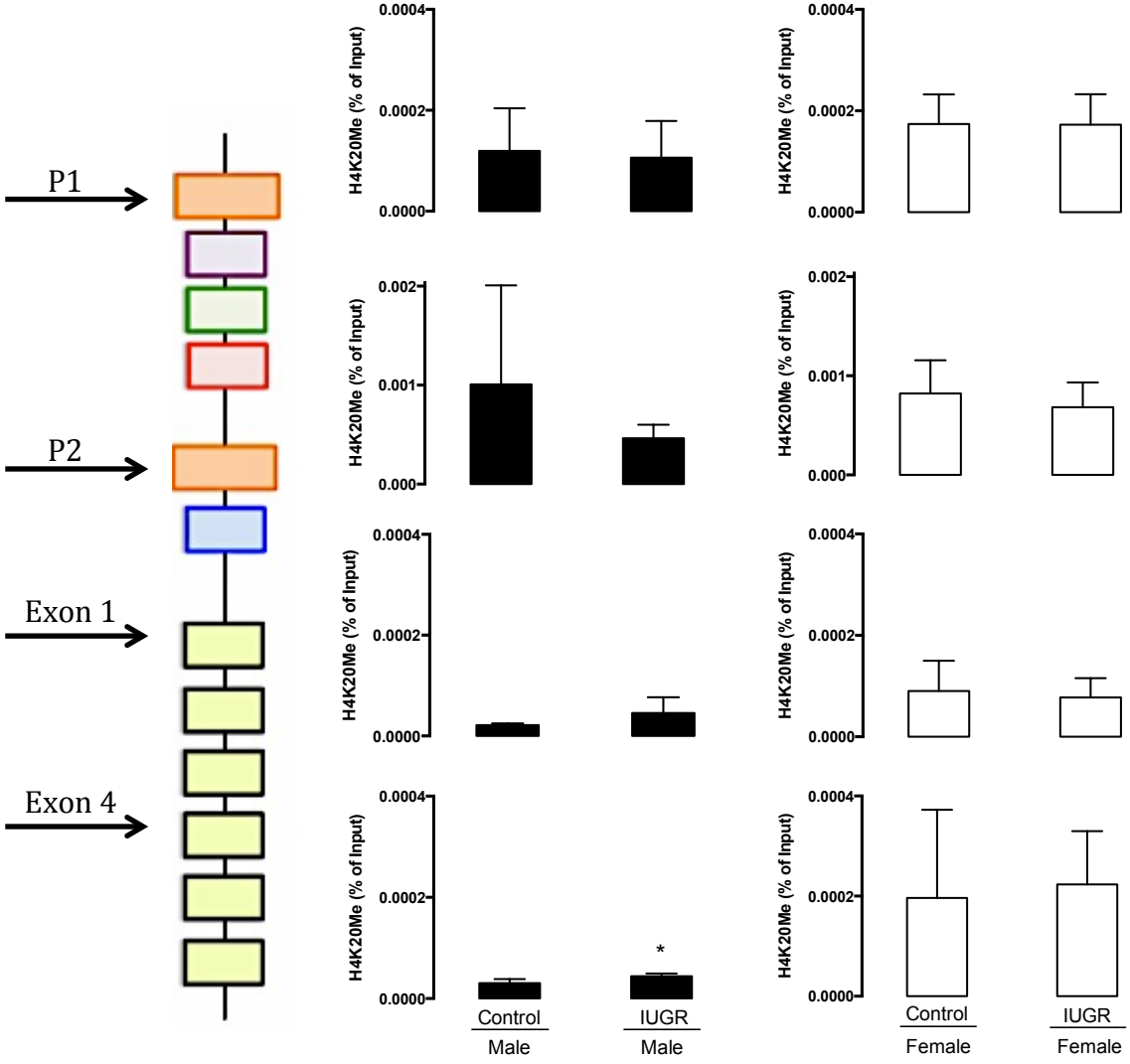

Figure 10 Effect of IUGR on H4K20Me along PPARγ
* Denotes statistical significance relative to sex-matched controls, $p \leq 0.05$.

DISCUSSION

The novel results of our study demonstrate that sex differences exist between basal levels of PPARγ2-Setd8-H4K20Me in male and female control rat pups. Our results also demonstrate that IUGR dysregulates the PPARγ2-Setd8-H4K20Me positive feedback loop in a sex-specific manner. The majority of molecular effects were confined to male rat pups, with female rat pups relatively unaffected. Importantly, the observed loop dysregulation and adipose dysfunction in male rats occurs *prior* to the onset of overt obesity, when IUGR rat pups still weigh significantly less than controls. These results suggest that, in male rats, IUGR programs altered adipose tissue gene expression and subsequent adipose dysfunction.

Our study showed important sex differences between control rat pups. Females had significantly higher PPARγ2 and Setd8 mRNA levels compared to males. Interestingly, both males and females had the highest levels of H4K20Me at P2 with less H4K20Me at P1, Exon 1, and Exon 4. However, females had significantly more H4K20Me at Exon 1 and Exon 4 along the PPARγ gene compared to males. In adipose cell lines, H4K20Me is associated with increased expression in 85% of the genes modified by the mark, suggesting a role in transcriptional activation (20). Furthermore, H4K20Me within the body of the gene has been suggested to promote elongation (20, 24). Increased levels of H4K20Me along the body of the gene in female rat pups may contribute to increased levels of PPARγ2 mRNA, thus increasing the propensity for SAT

expansion in females relative to males. Sex-specific programming of adipose tissue may play an important role in adipose differentiation and contribute to the varying responses to IUGR in male and female rat adipose tissue.

This sex-specific characterization at baseline is important because alterations in the PPARγ2-Setd8-H4K20Me loop are dependent on baseline levels. Furthermore, sex-specific responses have been demonstrated in both human and rodent obesity. In humans, women have been shown to accumulate more SAT while men accumulate more VAT (25). Similarly, in mice, females fed a high fat diet exhibit an increased capacity for adipocyte enlargement, as well as decreased macrophage infiltration, lower ectopic fat deposition in the liver, and later glucose tolerance impairment than male mice of the same age (26). Although sex-specific responses have been demonstrated in obesity, medicine has traditionally treated males and females equally. Our results provide further evidence that significant differences exist between baseline male and female control of gene expression and adipose regulation. Collectively, these findings have significant clinical relevance and provide additional support for the tailored medical treatment of males and females with the same disorder.

Our results expand upon the characterization of adipose dysfunction in IUGR rats. Adipose dysfunction is generally depicted by the overexpansion of adipocytes and the concomitant release of free fatty acids and pro-inflammatory signaling molecules (11). As a result, adipocytes lose their ability to efficiently sequester and store lipid. Thus, lipid is deposited ectopically in the liver, muscle, and VAT. However, activation of PPARγ2 results in adipocyte hyperplasia with a concurrent shift of lipid deposition back into SAT (27), the primary adipose storage depot. Results from this study show that IUGR

increases male SAT PPARγ2 mRNA levels, consistent with an attempt at SAT expansion. However, PPARγ2 protein levels do not significantly increase in parallel with the increase in PPARγ2 mRNA levels. In fact, cytoplasmic PPARγ2 protein levels are significantly decreased while total PPARγ2 protein levels remain unchanged in male IUGR rat SAT. However, in the face of no detectable increase in total PPARγ2 protein levels in male SAT, Setd8 mRNA levels still increase. This may be a result of increased PPARγ2 transcriptional activity on target genes, such as Setd8.

Setd8 is an important downstream target of PPARγ2 and a crucial regulator of the cell cycle. Precise modulation of Setd8 is essential for proper cell cycle progression (28), and cell cycle regulation is an important event in adipocyte differentiation (29). As an intermediate in the PPARγ2-Setd8-H4K20Me positive feedback loop, adequate Setd8 expression is necessary for controlled adipogenesis (20). In other cell types, deletion of Setd8 impairs both proliferation and differentiation processes (30). In our model, IUGR significantly increases Setd8 mRNA levels in male rat SAT, again suggesting an attempt at SAT expansion through increased proliferation and differentiation. However, Setd8 protein levels are not increased in parallel with increases in mRNA levels, and protein levels remain unchanged.

Our study demonstrated that PPARγ2 and Setd8 mRNA levels increase without a subsequent increase in protein in male IUGR rats. One explanation for this disconnect may be linked to the activation to the UPR. The UPR is a cell survival mechanism activated in response to cellular stress and accumulation of improperly folded protein products in the endoplasmic reticulum (ER) (31). One component of the UPR used to reduce the load on the ER is phosphorylation of eukaryotic translation initiator factor 2α

(eIF2α). Phosphorylation of eIF2α leads to global translation inhibition. Phosphorylation of eIF2α has previously been associated with lower PPARγ expression levels (30). We have previously shown that IUGR activates the UPR and increases the ratio of phosphorylated eIF2α (p-eIF2α) to unphosphorylated eIF2α in male rat SAT (15). We postulate that increased levels of p-eIF2α may inhibit PPARγ2 and Setd8 translation, preventing parallel increases in mRNA and protein levels. The inability to increase protein levels in parallel with changes in PPARγ2 and Setd8 mRNA may impair SAT differentiation and promote ectopic lipid deposition.

Interestingly, we showed that although Setd8 protein levels are unchanged in male IUGR rat SAT, levels of H4K20Me are increased at Exon 4 along the PPARγ2 gene. We postulate that selectively placed H4K20Me at Exon 4 along PPARγ2 may promote elongation and contribute to the increased PPARγ2 mRNA levels observed in male IUGR rat SAT.

Our study is not without limitations. In this study, we examined the effects of H4K20Me along the PPARγ gene; however, we did not examine how other target genes of Setd8 are affected. We also did not examine the PPARγ2-Setd8-H4K20Me loop in VAT secondary to limited materials. Our results suggest that a larger sample size is necessary to test for statistical significance in these measures. A larger sample size than expected is likely due to the difficult nature of working with adipose tissue. Lastly, no cause and effect conclusions can be made due to the descriptive nature of our work. Future studies testing cause and effect in adipose cell culture are warranted to better understand the relationships between the UPR and PPARγ and Setd8 translation inhibition, as well as the effect of altered Setd8 and H4K20Me on adipose differentiation.

In conclusion, the PPARγ2-Setd8-H4K20Me loop is sex dependent and is affected by IUGR in male adolescent rats. The increased H4K20Me found within the body of the PPARγ gene in female rats may drive increased PPARγ2 expression and contribute to the increased propensity for SAT expansion observed in female rats. Furthermore, our sex-specific molecular observations may partially explain the varying responses of male and female adipose tissue to IUGR.

APPENDIX

Table 1 Primer/Probe Sets for ChIP RT-PCR

Transcript position relative to PPARy gene	Sequence
Promoter 1 (P1)	Forward: AAAAACAAACTTCTGCGTGACAGT
	Reverse: GGTCCCACGTTCCTCAGACA
	Probe: AGGGCACCAGCCGG
Promoter 2 (P2)	Forward: CCAAGTCTTGCCAAAGAAGCA
	Reverse: GATTGAGAGCCAGCTGTGACAA
	Probe: ACAGCATTATGACACACCAT
Exon 1	Forward: CCCACCAACTTCGGAATCAG
	Reverse: GGAATGGGAGTGGTCATCCA
	Probe: TCTGTGGACCTCTCTG
Exon 4	Forward: CCATCAGGTTTGGGCGAAT
	Reverse: GATCTCCGCCAACAGCTTCT
	Probe: CCACAGGCCGAGAAG

REFERENCES

1. Fox CS, Massaro JM, Hoffmann U, Pou KM, Maurovich-Horvat P, Liu CY, Vasan RS, Murabito JM, Meigs JB, Cupples LA, et al. Abdominal visceral and subcutaneous adipose tissue compartments: association with metabolic risk factors in the Framingham Heart Study. Circulation 2007;116:39-48.

2. Rosenberg A. The IUGR newborn. Seminars in perinatology 2008;32:219-24.

3. Cetin I, Alvino G. Intrauterine growth restriction: implications for placental metabolism and transport. A review. Placenta 2009;30 Suppl A:S77-82.

4. Kinzler WL, Vintzileos AM. Fetal growth restriction: a modern approach. Curr Opin Obstet Gynecol 2008;20:125-31.

5. Kensara OA, Wootton SA, Phillips DI, Patel M, Jackson AA, Elia M. Fetal programming of body composition: relation between birth weight and body composition measured with dual-energy X-ray absorptiometry and anthropometric methods in older Englishmen. Am J Clin Nutr 2005;82:980-7.

6. Ong KK, Dunger DB. Birth weight, infant growth and insulin resistance. Eur J Endocrinol 2004;151 Suppl 3:U131-9.

7. Cottrell EC, Ozanne SE. Early life programming of obesity and metabolic disease. Physiology & behavior 2008;94:17-28.

8. Desai M, Beall M, Ross MG. Developmental origins of obesity: programmed adipogenesis. Curr Diab Rep 2013;13:27-33.

9. Ong KK, Ahmed ML, Emmett PM, Preece MA, Dunger DB. Association between postnatal catch-up growth and obesity in childhood: prospective cohort study. BMJ 2000;320:967-71.

10. Rasouli N, Molavi B, Elbein SC, Kern PA. Ectopic fat accumulation and metabolic syndrome. Diabetes Obes Metab 2007;9:1-10.

11. Hajer GR, van Haeften TW, Visseren FL. Adipose tissue dysfunction in obesity, diabetes, and vascular diseases. Eur Heart J 2008;29:2959-71.

12. Gregor MF, Hotamisligil GS. Thematic review series: Adipocyte Biology. Adipocyte stress: the endoplasmic reticulum and metabolic disease. J Lipid Res 2007;48:1905-14.

13. Uthaya S, Thomas EL, Hamilton G, Dore CJ, Bell J, Modi N. Altered adiposity after extremely preterm birth. Pediatr Res 2005;57:211-5.

14. Joss-Moore LA, Wang Y, Campbell MS, Moore B, Yu X, Callaway CW, McKnight RA, Desai M, Moyer-Mileur LJ, Lane RH. Uteroplacental insufficiency increases visceral adiposity and visceral adipose PPARgamma2 expression in male rat offspring prior to the onset of obesity. Early Hum Dev 2010;86:179-85.

15. Riddle ES, Campbell MS, Lang BY, Bierer R, Wang Y, Bagley HN, Joss-Moore L. Intrauterine Growth Restricion Increases TNFα and Activates the Unfolded Protein Response in Male Rat Pups. Journal of Obesity (In Review). 2014.

16. Lane RH, Kelley DE, Ritov VH, Tsirka AE, Gruetzmacher EM. Altered expression and function of mitochondrial beta-oxidation enzymes in juvenile intrauterine-growth-retarded rat skeletal muscle. Pediatr Res 2001;50:83-90.

17. McMullen S, Langley-Evans SC, Gambling L, Lang C, Swali A, McArdle HJ. A common cause for a common phenotype: the gatekeeper hypothesis in fetal programming. Med Hypotheses 2012;78:88-94.

18. Fajas L, Auboeuf D, Raspe E, Schoonjans K, Lefebvre AM, Saladin R, Najib J, Laville M, Fruchart JC, Deeb S, Vidal-Puig A, et al. The organization, promoter analysis, and expression of the human PPARgamma gene. The Journal of biological chemistry 1997;272:18779-89.

19. Ferre P. The biology of peroxisome proliferator-activated receptors: relationship with lipid metabolism and insulin sensitivity. Diabetes. 2004;53 Suppl 1:S43-50.

20. Wakabayashi K, Okamura M, Tsutsumi S, Nishikawa NS, Tanaka T, Sakakibara I, Kitakami J, Ihara S, Hashimoto Y, Hamakubo T, et al. The peroxisome proliferator-activated receptor gamma/retinoid X receptor alpha heterodimer targets the histone modification enzyme PR-Set7/Setd8 gene and regulates adipogenesis through a positive feedback loop. Mol Cell Biol 2009;29:3544-55.

21. Guiding principles for research involving animals and human beings. Am J Physiol Regul Integr Comp Physiol 2002;283:R281-3.

22. Livak KJ, Schmittgen TD. Analysis of relative gene expression data using real-time quantitative PCR and the 2(-Delta Delta C(T)) Method. Methods 2001;25:402-8.

23. Nelson JD, Denisenko O, Bomsztyk K. Protocol for the fast chromatin immunoprecipitation (ChIP) method. Nat Protoc 2006;1:179-85.

24. Barski A, Cuddapah S, Cui K, Roh TY, Schones DE, Wang Z, Wei G, Chepelev I, Zhao K. High-resolution profiling of histone methylations in the human genome. Cell 2007;129:823-37.

25. Lovejoy JC, Sainsbury A. Sex differences in obesity and the regulation of energy homeostasis. Obes Rev 2009;10:154-67.

26. Medrikova D, Jilkova ZM, Bardova K, Janovska P, Rossmeisl M, Kopecky J. Sex differences during the course of diet-induced obesity in mice: adipose tissue expandability and glycemic control. Int J Obes (Lond) 2012;36:262-72.

27. Kim JY, van de Wall E, Laplante M, Azzara A, Trujillo ME, Hofmann SM, Schraw T, Durand JL, Li H, Li G, Jelicks LA, et al. Obesity-associated improvements in metabolic profile through expansion of adipose tissue. The Journal of clinical investigation 2007;117:2621-37.

28. Wu S, Rice JC. A new regulator of the cell cycle: the PR-Set7 histone methyltransferase. Cell Cycle 2011;10:68-72.

29. Tang QQ, Otto TC, Lane MD. Mitotic clonal expansion: a synchronous process required for adipogenesis. Proc Natl Acad Sci USA 2003;100:44-9.

30. Driskell I, Oda H, Blanco S, Nascimento E, Humphreys P, Frye M. The histone methyltransferase Setd8 acts in concert with c-Myc and is required to maintain skin. Embo J 2012;31:616-29.

31. Hetz C. The unfolded protein response: controlling cell fate decisions under ER stress and beyond. Nat Rev Mol Cell Biol 2012;13:89-102.